XVII. COMPUTER COMPONENTS AND SYSTEMS[*]

Dr. E. W. Fletcher J. M. Ballantyne A. H. Nelson
Prof. A. L. Loeb   R. Casale   S. B. Russell
Prof. C. C. Robinson C. K. Crawford F. W. Sarles, Jr.
         T. More, Jr.

A. FUNDAMENTAL PHYSICS OF THE THIN-FILM STATE

1. MAGNETO-OPTIC EFFECTS IN FERROMAGNETIC THIN FILMS

If a ferromagnetic thin film is magnetized in a direction longitudinal to the plane of incidence, there is a magnetically induced change in the polarization of the reflected and the transmitted light. When the incident light is plane polarized in the plane of incidence, a second component appears in the reflected and the transmitted beams perpendicular to the plane of incidence. Thus, the incident plane-polarized light is reflected and transmitted elliptically polarized, with the azimuth of the major axis of the ellipse rotated slightly away from the plane of incidence. By a reversal of the magnetization of the film, the sign of the ellipticity is changed and the major axis is rotated symmetrically to the other side of the plane of incidence. The polarization change in the reflected beam is called the "Longitudinal Kerr Effect," and, for lack of a better name, the change in the transmitted beam will be called the "Longitudinal Faraday Effect." The former effect has been discussed at length in previous reports; in the present report only the theory for the longitudinal Faraday effect will be covered.

The film configuration for which the derivation was made is shown in Fig. XVII-1.
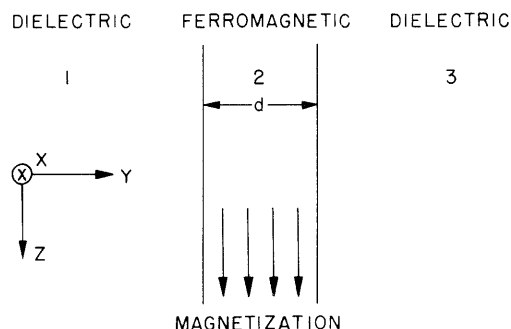

Fig. XVII-1. A ferromagnetic thin film between two dielectrics.

The amplitude of the electric field obliquely incident on the ferromagnetic from medium 1 is I, and the amplitude of the electric field transmitted into medium 3 is T, and subscripts p and s refer to a component plane polarized in the p or s direction. The form

---

of the transmission coefficients is, then,

$$T_p = t_{pp} I_p + t_{ps} I_s \tag{1}$$

$$T_s = t_{sp} I_p + t_{ss} I_s \tag{2}$$

The coefficients t_{pp} and t_{ss} are the ordinary transmission coefficients associated with an unmagnetized metallic film and are evaluated in the conventional manner. Their form is shown in the following equations.

$$t_{pp} = \frac{t_{12_p} t_{23_p} e^{-j\rho/2}}{1 - r_{23_p} r_{21_s} e^{-j\rho}} \tag{3}$$

$$t_{ss} = \frac{t_{12_s} t_{23_s} e^{-j\rho/2}}{1 - r_{23_s} r_{21_s} e^{-j\rho}} \tag{4}$$

where

$$\rho = \frac{4\pi d \cos \phi_2}{\lambda_o} \tag{5}$$

In Eqs. 3, 4, and 5, the t's and r's are the transmission and reflections coefficients at the interfaces designated by the subscripts under the conditions that both media are infinitely thick. The light is incident from the medium given by the first subscript. (Any optics textbook will supply these coefficients.)

By following a similar procedure, the Faraday transmission coefficients are found to be:

$$t_{ps} = \frac{t_{12_s} t_{23_{ps}} e^{-j\rho/2}}{1 - r_{23_p} r_{21_s} e^{-j\rho}} \tag{6}$$

$$t_{sp} = \frac{t_{12_p} t_{23_{sp}} e^{-j\rho/2}}{1 - r_{23_p} r_{21_p} e^{-j\rho}} \tag{7}$$

In Eqs. 6 and 7 the transmission coefficients with the double-letter subscripts provide the change in polarization with magnetization and are the source of the magneto-optic effect. Expressions for the magneto-optic coefficients $t_{23_{ps}}$ and $t_{23_{sp}}$ are given by

$$t_{ps} = i \frac{Q \sin \phi_2 \cos \phi_2}{\cos \phi_1} \left[\frac{Z_{z_1}}{Z_{z_1} + Z_{z_2}} + \frac{\left(Z_{x_3} - Z_{x_2}\right)}{\left(Z_{x_3} + Z_{x_2}\right)} \frac{Z_{z_3}}{\left(Z_{z_3} + Z_{z_2}\right)} \right.$$

$$\left. + \frac{Z_{z_2} + Z_{z_1}}{\left(Z_{z_1} + Z_{z_3}\right)\left(Z_{z_3} + Z_{z_2}\right)} + \frac{2\pi d}{\lambda} \frac{Z_{z_3}}{Z_{z_3} + Z_{z_2}} \right] \tag{8}$$

$$t_{sp} = -iQ \frac{\sin \phi_2 \cos \phi_1}{\cos \phi_2} \left[\left\{ \frac{Z_{x_1}}{Z_{x_1} + Z_{x_2}} - \frac{Z_{x_1} + Z_{x_3}}{\left(Z_{x_2} + Z_{x_3}\right)\left(Z_{x_1} + Z_{x_2}\right)} \right. \right.$$

$$\left. \left. - \frac{\left(Z_{z_3} - Z_{z_2}\right)}{\left(Z_{z_3} + Z_{z_2}\right)} \frac{Z_{x_2}}{Z_{x_2} + Z_{x_3}} \right\} \frac{1}{\cos^2 \phi_2} + \frac{2\pi d}{\lambda} \frac{Z_{x_2}}{Z_{x_2} + Z_{x_3}} \right] \tag{9}$$

where

$$Z_x = \frac{1}{N \cos \phi} \left(\frac{u_o}{\epsilon_o} \right)^{1/2}$$

$$Z_z = \frac{\cos \phi}{N} \left(\frac{u_o}{\epsilon_o} \right)^{1/2}$$

In these expressions, N with the proper subscript is the index of refraction of the medium in question (N_2 will be complex). The angle ϕ is the angle between the direction of propagation and the y-axis and is assigned a subscript according to the medium traversed. The letter Q is the complex magneto-optic amplitude that was first introduced by Voigt and applies only to the ferromagnetic film.

This derivation is based on the assumption that only the first few internal reflections of a light ray affect the transmission through the film. For films thicker than 1/8 of a wavelength, this approximation should be quite valid.

C. C. Robinson

2. DIELECTRIC FILMS FORMED BY DECOMPOSITION

The electron gun previously used for metallic deposition (1, 2) has been used to form dielectric layers by electron-impact decomposition of tetraethoxysilane. This deposition method has been used by others (3, 4, 5) to make thin insulating films for etching processes and tunneling devices.

Three-layer (gold-dielectric-gold) capacitors were made in order to determine some of the dielectric properties of these insulating films. In this experiment, 1200 ev

electrons with a substrate current density of approximately $1/10$ ma/cc^2 were used to decompose the absorbed layers of the silane vapor. A 20-minute exposure at 1 μ Hg total pressure, as measured by a conventional ionization gauge, was used. Dissipation factors of approximately 50 per cent which were found on 5 runs suggest that a high carbon deposition is taking place along with the desired silicon-oxygen film deposition. It is still not known whether the carbon is coming from the ethyl radicals, or from the decomposition of organic contaminents present in the system.

Under the most ideal conditions, it should be possible to break the ethyl bonds and leave only Si, O combinations on the substrate. Such a film should have excellent dielectric properties. To do this, an energy source that is above the ethyl radical bond energy level, but below the bond energies holding the radical together, is needed. With the high-energy sources that are being used it is thought that a polymerization process (3, 4) occurs and gives films composed of C, H, O, Si. Other experiments show, however, that the use of very low-energy beams, (energies below the first secondary emission crossover of the substrate-dielectric film combination) is, perhaps, impractical because of charging effects that cut off the beam.

From this work and from the work of Christy (4), it is concluded that dielectric films can be made that will be useful for field emission devices and other applications.

A. G. Baker, J. R. Ellis, Jr.

(Mr. Allen G. Baker is now at Lincoln Laboratory, M. I. T.)

References

1. A. G. Baker and W. C. Morris, Deposition of metallic films by electron impact decomposition of organometallic vapors, Rev. Sci. Instr. 32, 458 (1961).

2. E. W. Fletcher, A. G. Baker, and W. C. Morris, Electron decomposition plating, First Joint Progress Report of the Laboratories for Molecular Science and Molecular Engineering, M. I. T., January 1961, p. 159.

3. D. A. Buck and K. R. Shoulders, An approach to microminiature printed systems, a paper presented at the Eastern Joint Computer Conference, Philadelphia, December 1958.

4. R. W. Christy, J. Appl. Phys. 31, 1680-1683 (1960).

5. It has come to our attention that I. Giaever, of General Electric Research Laboratories, Schenectady, New York, has done some work in this field.

3. METALLIC FILMS FORMED BY DECOMPOSITION

Metallic films of Pb and Sn made by the electron-beam decomposition method described by Fletcher, Baker, and Morris(1)are thought to have a high carbon content. Some of the films had a brown appearance, while others had bright metallic appearances. It is thought that the carbon deposition is due to the decomposition of residual organic vapor in the vacuum system, and/or from the actual decomposition of the ethyl, methyl or

butyl radicals (1). The electron energies used in the initial experiments were approximately 1 KCV; however, the radical bonding energies are only a few volts.

In order to have an operation that is such that only the radical-to-metal bond would be broken, a secondary emission source was tried. A 1-KV electron beam was allowed to strike a copper plate at a 60° angle to the normal. A glass substrate with a stainless steel mask was placed parallel to the copper plate, approximately 2 cm above the striking point on the plate.

Nearly 90 per cent of the secondary electrons are usually found to be in the region 0-10 volts with only approximately 3 per cent near the primary beam energy, and a nearly cosine distribution is found to exist (2). For tetra-butyl tin, with a 20-minute run at 1 μ, a metallic film, estimated to be approximately 400 $\overset{\circ}{A}$ thick, was deposited on the metal mask, whereas no observable deposit was formed on the glass substrate. The glass surface probably attained a negative charge that enfeebled the striking beam current.

It can be seen that additional experiments should be made with low-energy electrons and metallic substrates.

A. G. Baker

References

1. E. W. Fletcher, A. G. Baker, and W. C. Morris, Electron decomposition plating, First Joint Progress Report of the Laboratories for Molecular Science and Molecular Engineering, M.I.T., January 1961, p. 159.

2. K. R. Spangenberg, Vacuum Tubes (McGraw-Hill Book Company, New York, 1948), p. 52.

B. CRYSTAL ALGEBRA

The structures analyzed thus far appear to fall into the following classes:

A. Structures derived from stacked hexagonal nets.

    A1. Cubically stacked nets.

    A2. Hexagonally stacked nets.

    A3. Hexagonal nets stacked otherwise.

B. Structures not derived from stacked hexagonal nets.

For each of these classes, algorithms have been derived for locating all possible sites; and for each structure analyzed, a distribution pattern has been derived to describe the location or absence of ions at all sites.

Examples of structures previously reported on are:

A1: Rocksalt, Sphalerite, Spinel, Cesium Chloride, Perovskite;

A2: Nickel Arsenide, Wurtzite, Olivine;

A3: Quartz; and

B: Rutile.

In the Quarterly Progress Report No. 61 (pages 270-274) the calcium silicide structure was discussed. This structure, which belongs to class A3, will be dealt with further in the present report; other silicides belonging to A3 are also included. Finally, two structures of class A1 will be discussed.

a. The Calcium Silicide Structure

In the previous quarterly report, all possible ways were considered of stacking close-packed calcium nets and silicon nets conforming to the Ca- and Si-environments. It was found that there are only two distinct stacking modes: one that would correspond to a polar structure and a small period along the hexagonal axis, and another that corresponds to a nonpolar structure, having a larger period. Comparison of these structures with experimental observations indicates that the latter stacking mode is the one that corresponds to the naturally occurring calcium silicide structure.

The following algorithm has accordingly been derived for the description of the calcium silicide structure:

$$\text{Ca at} \quad h = 5k + 2$$

$$\text{Si at} \begin{cases} h = 5k \\ h = 5k + 4 \end{cases}$$

where k is an integer.

The location of the ions in each h-plane is given by

$$v = 3L + \left[f(h, k)\right]_{\text{mod } 3}$$

$$w = 3M + \left[f(h, k)\right]_{\text{mod } 3}$$

$$f(h, k) = \frac{1}{2}h - 2k_{\text{mod } 6} - \frac{1}{2}k_{\text{mod } 2}$$

b. The Titanium, Chromium, and Molybdenum Silicide Structures

In these structures each hexagonal net is occupied by both elements. As is the case with quartz, the hexagonal nets are stacked directly above each other (f(h) = constant), but the description of the occupied sites requires subdivision into twelve subarrays (1,2). In terms of the notation described in these reports, the three structures are coded as shown in Table XVII-1. It is observed that these three structures differ from each other in the variety of combinations represented, in a manner similar to the distinction between hexagonal and cubic close packing.

Table XVII-1. Distribution patterns for three silicides.

TiSi$_2$		CrSi$_2$		MoSi$_2$	
Ti:	Si:	Cr:	Si:	Mo:	Si:
ap	a(q⊕r)	ap	a(q⊕r)	ap	a(q⊕r)
cp	c(q⊕r)	cp	c(q⊕r)	bp	b(q⊕r)
dp	d(q⊕r)	bp	b(q⊕r)		
bp	b(q⊕r)				

c. Stannite and Chalcopyrite

The structures just discussed can all be built with the aid of the hexagonal-net modu-ledra (3). We have also returned to the study of class Al, and are considering two structures that can be represented by proper stacking of tetrahedral and octahedral interstitial moduledra. Since these models are now available in a variety of colors, it is possible to use them for structures in which anions are (cubically or hexagonally) close packed, and in which several different cations occupy the same h-plane. Two such structures are stannite (Cu$_2$FeSnS$_4$) and chalcopyrite (CuFeS$_2$). Both of these structures are derivatives of sphalerite (ZnS), with zinc appropriately replaced by copper, iron, and tin ions. In sphalerite, one-half of all of the tetrahedral sites is occupied by zinc; in chalcopyrite, one-quarter is occupied by copper, and one-quarter by iron, while in stannite one-quarter of all of the tetrahedral sites is occupied by copper, one-eighth by tin, and one-eighth by iron. Both of these structures are now being built with the aid of moduledra, and their distribution patterns are being derived.

A. L. Loeb

References

1. A. L. Loeb, Subdivision of hexagonal arrays, High Speed Computer System Research, Quarterly Progress Report No. 10, Computer Components and Systems Group, M. I. T., 30 April 1960, pp. 26-31.

2. A. L. Loeb, Topology of Structures, High Speed Computer System Research, Quarterly Progress Report No. 11, op. cit., 31 July 1960, pp. 18-19.

3. Ibid., loc. cit.